BioNanoScience (2018) 8:587–595
https://doi.org/10.1007/s12668-018-0514-7

ZnO Nanoparticles with Different Sizes and Morphologies for Medical Implant Coatings: Synthesis and Cytotoxicity

B. C. Costa[1,2] · E. A. Rodrigues[3] · C. K. Tokuhara[2,4] · R. C. Oliveira[2,4] · P. N. Lisboa-Filho[2,5] · L. A. Rocha[2,5]

Published online: 3 March 2018
© Springer Science+Business Media, LLC, part of Springer Nature 2018

Abstract
Zinc oxide (ZnO) has been used in a large range of technological applications, from light-emitting diodes (LEDs) and solar cells to cancer diagnosis and treatment agents. In the last decades, however, a novel antimicrobial property for ZnO particles has been explored, making this oxide an interesting material to be incorporated or deposited on biomaterials, for example in coatings over metallic implants. In this scenario, ZnO physico-chemical properties, mainly particles' size and morphology, will play fundamental role on its performance. Thus, in this work, two different procedures of a chemical synthesis route named sonochemistry were used to achieve different morphologies/sizes of ZnO. Then, the obtained particles were used to evaluate possible cytotoxic effects against MC3T3-E1 mouse pre-osteoblasts (bone cells). The obtained results indicated that the sonochemical route is an effective way to produce different ZnO morphologies and the way in which these particles interact with osteoblasts (directly or indirectly) may completely influence their cytotoxicity.

Keywords Zinc oxide · Sonochemistry · Cytotoxicity · Biomaterials · Coatings

1 Introduction

Zinc oxide (ZnO) is a widely recognized material target of several studies around the world due to its unique properties. Among its main characteristics, the high electronic mobility, high thermal conductivity, wide and direct band gap (3.37 eV at room temperature), and large exciton-binding energy (60 meV) have gained the most interest for diverse applications [1, 2]. In fact, such properties make this oxide suitable for a wide range of technological applications, including transparent thin film transistors, photodetectors, light-emitting diodes, laser diodes, gas sensors, varistors, transducers, solar cells, and compact cold cathodes, among many others [1, 2].

More recently, however, this oxide has been investigated to be used in biomedical devices and materials, due to high chemical stability and recognized antibacterial activity. Furthermore, ZnO also presents potential application as drug carrier and biosensor for diagnosis and cancer treatment [3–8].

In addition to its antibacterial properties, ZnO has been used as coatings in metallic orthopedic and dental implants, since zinc may increase bone formation, stimulating osteoblast (bone cells) activity and cell proliferation. Furthermore, zinc is also considered a cofactor for collagen synthesis and a supporting element for several enzymes, particularly alkaline phosphatase, involved in bone mineralization [9, 10].

For decades, one of the most common elements used as an antibacterial agent in biomedical materials was silver (Ag), presenting high efficiency against a broad spectrum of bacteria (both *gram-positive* and *-negative*). However, this element presents a wide range of controversial reports regarding its cytotoxicity in osteoblast cells, being able to affect basic

✉ B. C. Costa
brunah@fc.unesp.br

[1] Graduate Program in Materials Science and Technology – POSMAT, São Paulo State University – UNESP, Av. Eng. Luiz Edmundo Carrijo Coube 14-01, Bauru, SP 17033-360, Brazil

[2] Brazilian Branch of the Institute of Biomaterials, Tribocorrosion and Nanomedicine – IBTN/Br, Av. Eng. Luiz Edmundo Carrijo Coube 14-01, Bauru, SP 17033-360, Brazil

[3] Department of Biological Sciences, São Paulo State University – UNESP, Av. Eng. Luiz Edmundo Carrijo Coube 14-01, Bauru, SP 17033-360, Brazil

[4] Bauru School of Dentistry, University of São Paulo – USP, Alemeda Dr. Otávio Pinheiro Brisolla, 9-75, Bauru, SP 17012-901, Brazil

[5] Department of Physics, São Paulo State University – UNESP, Av. Eng. Luiz Edmundo Carrijo Coube 14-01, Bauru, SP 17033-360, Brazil

cellular metabolic functions, as well as to be deposited and accumulated in the blood or several organs [11].

Although easily deposited over metallic implant surfaces, mainly titanium implants [12, 13], Ag-containing surface coatings may suffer from corrosion and wear processes, leading to the release of ions and nanoparticles (NPs) [14]. Particularly, high rates of Ag ion release may have negative effects over osteoblasts' and osteoclasts' cell differentiation and viability [15]. Furthermore, regarding Ag NPs, size appears to be the most important factor in the interaction with human cells, with smaller Ag NPs being able to go through the plasmatic membranes, internalizing the cells, provoking even more cytotoxic effects [16].

In this context, ZnO-based biomaterials emerge as an interesting alternative to Ag coatings over metallic implant surfaces and in many other biomedical devices. In contrast to other metal oxides, ZnO is considered biocompatible for several applications. Although, in the mesoscale, some studies indicate relevant toxicity for the liver, spleen, heart, pancreas, and bone tissues, no consensual opinion exists [17, 18].

According to some studies, the antibacterial mechanism of ZnO is associated with the possible accumulation or deposition of ZnO NPs in the membrane or cytoplasm of bacteria, leading to bacteriostatic and bactericidal effects [19]. Additionally, a recent work has demonstrated that different metals, including zinc, may cause negative effects in bacterial cells via protein-dysfunction and membrane-damage processes [20]. However, the most recognized mechanism for the antibacterial activity of ZnO is reactive oxygen species (ROS) production, namely hydroxyl radicals and the increase of oxidative stress [3].

Another important issue to be considered regarding ZnO bacterial toxicity is that there is a direct relation between biological activity and the size and shape of ZnO nanostructures. The size may influence the cellular internalization of the ZnO NPs and bacterial damages to the cells. Additionally, although size effects are directly associated with surface area, it seems that shape presents a relevant capability to induce toxicity. As well, it appears that there is also a connection between particle size and intracellular reactive oxygen generation [21, 22].

Although it is definitely an interesting alternative for incorporation or improvement in the antibacterial potential on implant surfaces, it is important to emphasize that the use of this oxide for such application should also take into account its interaction with tissue cells adjacent to an implant in vivo (bone), with no deleterious effects.

Zinc's incorporation in biomedical materials with osteoconductive and repair proposals, such as hydroxyapatite (HAp), for example, appears to have a beneficial effect on osteoblasts (bone cells) proliferation and differentiation as well as a significant decrease in the osteoclast (bone cells responsible for bone resorption) number and in their resorptive activity, also demonstrating a strong decrease in the number of bacteria when compared with simple HAp [23–25]. Moreover, specifically regarding the zinc incorporated on titanium dioxide porous coatings over metallic surfaces, it may effectively inhibit bacterial growth due to the slow and constant zinc ions' release from the coatings, showing an enhancement in the adhesion, proliferation, and differentiation of bone-marrow mesenchymal stem cells in the oxide surface, without cytotoxic effects [26].

Therefore, considering that ZnO's incorporation in surface coatings of ceramic or metallic materials may improve its bioactivity (being less harmful than Ag particles regarding bone cells function and proliferation) and enhance its behavior regarding bacterial infection and taking into account that size and morphology of the incorporated ZnO NPs play key roles in these bioengineered surfaces performance, there is a wide range of possibilities to be explored and tested when studying the new nanostructures' physico-chemical and biological properties, as well as new ways to achieve and control such nanostructures' characteristics and properties.

An effective chemical route to produce different ZnO morphologies is the sonochemical method, although this method is poorly explored [27]. The sonochemical method consists of a chemical and ultrasound association and allows the preparation of a large variety of nanostructured materials, wherein the chemical effects arise from acoustic cavitation, a phenomenon that can be understood as a process consisting of the formation, growth, and implosive collapse of bubbles (with a lifetime of microseconds) in a liquid, wherein, temperatures up to 5000 °C and pressures of 1000 atm in located points may be achieved, leading to high-energy chemical reactions. Furthermore, acoustic cavitation concentrates the diffused ultrasound energy to a single set of conditions, providing materials with unique properties from their precursors dissolved in solution [28].

The sonochemical method is a simple, low-temperature, and environmentally friendly technique controlled by parameters including the amplitude and frequency of applied sound field, temperature, density of nuclei in solution, and probe-emitting radiation geometry [29]. Furthermore, according to Jung and co-workers, the control of other parameters, such as the type and concentration of precursors in solution and the power and time of ultrasonic irradiation may lead to different morphologies, such as nanoflowers, nanorods, nanospheres, nanodisks, and nanocups [27]. Studies carried out by different authors corroborate this idea, wherein octahedral [30] and ellipsoidal [31] NPs and porous nanospheres [32] were achieved.

Lastly, the sonochemical method may also promote morphological and structural modifications, as previously verified in our group, wherein high-power ultrasonic irradiation has promoted the emergence of an amorphous shell around ZnO NPs [33] and a recrystallization process in low-power synthesized ZnO mesostructures [34].

In this context, considering the well-recognized antibacterial properties of ZnO particles, their potential application in implants' coatings and the importance to evaluate their

harmful effects regarding living cells related to this application (mainly bone cells), ZnO structures with different sizes and morphologies were synthesized using the sonochemical method and evaluated to determine whether they are cytotoxic regarding MC3T3-E1 mouse pre-osteoblasts (bone cells) through two different approaches for in vitro assays (direct contact and non-contact).

2 Materials and Methods

2.1 Synthesis

Two different morphologies were synthesized using the sonochemical method, according to the methodology proposed by Jung and co-workers [14]. Thereunto, two equal solutions consisting in 4 g of zinc nitrate hexahydrate ($Zn(NO_3)_2$. $6H_2O$ P.A.—Vetec) dissolved in 300 ml of deionized water were prepared at room temperature. The pH of these solutions was then adjusted to 10 with the addition of 9 ml of ammonium hydroxide (NH_4OH, Impex). After dissolution, both above-described solutions were submitted to a sonochemical treatment for 60 min (5-min pulses with 1 min of pause) in a Sonics VCX-750 ultrasonic processor (20 kHz and 750 W) using an amplitude of 70% and/or an effective power of 45 W.

After sonication, the obtained precipitates for the first solution were immediately collected and washed five times in isopropyl alcohol and five times in deionized water using a centrifugal Hermle Labortechnik model Z-326, for 15-min cycles at 12.000 rpm. Lastly, the washed precipitates were dried in a vacuum oven at 100 °C for 2 h, and the resultant sample was named NP1. On the other hand, the precipitates obtained in the second sonochemically treated solution were collected only after 24 h, washed, and dried as mentioned above for the NP1 sample, and then, the obtained powder was named NP2. A third sample, which was named NP3, was also considered for this work as the standard for comparison, and it refers to the ZnO commercial powder (purchased from Aldrich, purity 99.999%) with no additional treatment.

Table 1 summarizes the synthesis conditions for each sample as well as its respective nomenclatures.

Table 1 Sample labels and synthesis conditions

Name	Sonication time (min)	Precipitation time
NP1	60	2 min
NP2	60	24 h
NP3* (commercial)	–	–

*No treatment was applied to the ZnO commercial powder (NP3 sample)

2.2 Physico-chemical Characterization

The crystallographic structure of the NP1, NP2, and NP3 samples was evaluated by X-ray diffraction (XRD) in a diffractometer Rigaku, D/MAX 2100 PC model, using CuKα radiation, 40 kV voltage, 20 mA current, a divergence slit of 1°, a receiving slit of 0.3 mm, nickel filter, in a 20 to 100° angular scan range, and a 0.02° step with fixed time of 1.6 s/step. The theoretical card PDF 36-1451, related to the ZnO hexagonal phase, was used to index all the obtained diffraction patterns. Additionally, morphological and dimensional analyses were carried out by scanning electron microscopy (SEM) using a JEOL microscope model 7500F with a theoretical resolution of 1 nm and 2 kV of acceleration voltage.

2.3 Cell Culture and Cell Viability Assay (MTT Reduction)

The MC3T3-E1 cell line (from ATCC—*American Type Culture Collections, subclone 14, CRL-2594*) of mouse pre-osteoblasts was cultured in α-MEM (Gibco) supplemented with 10% fetal bovine serum, (FBS, Gibco) and 1% penicillin/streptomycin (Gibco) at 37 °C and 5% CO_2 environment. Thereafter, before reaching confluence, cells were detached by trypsinization (trypsin purchased from Sigma-Aldrich), treated with trypan blue and counted in a hemocytometer [35].

Three different concentrations for each sample (synthetic or commercial ZnO powder/cell culture medium) were chosen to be tested in MC3T3 mouse pre-osteoblasts: 5, 10, and 50 μg/mL. Further, in this experiment, only cell culture medium supplemented with FBS 10% and antibiotics was used as control group. The chosen concentrations and models [36, 37] follow the recommended international standards ISO 10993-5:2009 [38] and ISO 10993-12:2012 [39]. In vitro cytotoxicity tests allow the employment of relevant cell types and lineages, using simple, controlled, and reproducible test conditions, and in conformity with the principles of bioethics [37, 38].

For cell viability tests, NP1, NP2, and NP3 samples were diluted in α-MEM culture cell medium in stock solutions with an initial concentration of 50 μg/mL to obtain the extracts (or conditioned medium). Then, the stock solutions were incubated for 48 h at 37 °C in a 5% CO_2 atmosphere for the complete precipitation of the ZnO particles. Simultaneously, 2×10^3 cells were cultured in the wells of a 96-well plate and incubated for 48 h at 37 °C and a 5% CO_2 atmosphere.

After 48 h, the culture medium of the cultured 96-well plates was removed and replaced by the extracts (or conditioned medium), obtained from the serial dilution of the ZnO stock solutions for the final chosen concentrations (50, 10, and 5 μg/mL).

Two different methodologies were adopted to investigate the cytotoxicity of ZnO NPs. First, only the supernatant was collected, separated from the ZnO precipitate, and filtrated (0.22-μm filter) to be used as extracts, before the serial dilution of the stock solutions. This methodology was assumed to avoid the direct contact of the ZnO powders with cells and to study the ionic cytotoxicity. In a second protocol, the cell culture medium containing the ZnO NPs was re-dispersed after 48 h of incubation and then serially diluted and used as extract. This methodology was used to investigate the effect of the direct contact of ZnO NPs with pre-osteoblast cells.

Moreover, cell viability was assessed for three periods of time: 24, 48, and 72 h, and the experiments were conducted at least in triplicate. After each experimental period, the extracts were removed, and cells were washed with PBS before an MTT (3-(4,5-dimethyltiazol-2-yl)-2,5-diphenyltetrazolium bromide) reduction test.

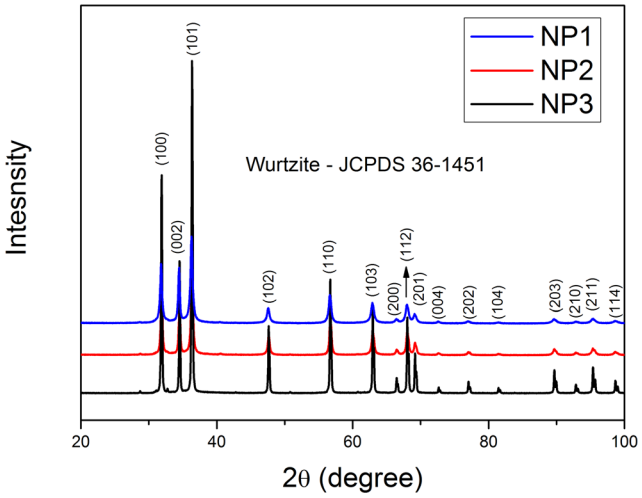

Fig. 1 Powder diffraction patterns for the samples NP1 (blue), NP2 (red), and NP3 (black)

3 Results

Figure 1 shows the obtained diffraction patterns for the three studied samples: NP1, NP2, and NP3. Accordingly, it is possible to point that all samples can be indexed as a ZnO hexagonal phase (Wurtzite—JCPDS 36-1451) without evident secondary phases. Furthermore, this figure illustrates that the synthesized ZnO samples, NP1 and NP2, present broader and less intense peaks than the ZnO commercial powder, NP3, demonstrating that the synthesized samples have less crystallinity than the commercial ZnO.

Figure 2a–f shows the obtained SEM images for the NP1, NP2, and NP3 samples.

Figure 2 demonstrates that the three studied samples present different morphologies and size distribution. According to Fig. 2a, b, the NP1 sample shows a rod-like morphology, with an average size of 360 ± 40 nm in length and 75 ± 20 nm in diameter. The NP2 sample (Fig. 2c) presents a flower-like morphology, presenting structures with sizes ranging from 500 to 900 nm and a calculated average size of 720 ± 100 nm. Additionally, for the NP2 sample, the obtained flower-like morphology is composed of smaller rod-like structures, as shown in Fig. 2d, which corresponds to the NP2 sample in detail. Lastly, the NP3 sample, shown in Fig. 2e, f, presents a regular and polygonal morphology (that may be approximated to parallelepipeds), in which it is possible to identify particles ranging from 200 nm to 2 μm, with a calculated average size of 560 ± 130 nm. Table 2 summarizes the calculated average size for the NP1, NP2, and NP3 samples and its respective standard deviations.

The obtained results for MTT assay, as a function of the type of NPs and concentration, are shown in Fig. 3. MTT allows the ionic cytotoxicity of ZnO NPs to be assessed. In fact, a non-contact protocol was adopted, collecting and filtering only the supernatant of the cell culture medium incubated with the ZnO NPs, avoiding direct contact with pre-osteoblast cells. In this figure, the symbols * for $p < 0.05$, ** for $p < 0.001$, and *** for $p < 0.0001$ were used.

According to the MTT results shown in Fig. 3, for 24 h, no significant and statistical differences for MC3T3-E1 cell viability were observed between any experimental groups. For 48 h, there is a slight increase in cell viability for the lower concentration (5 μg/mL) of the NP1 and NP3 groups, while a slight decrease for the higher concentration (50 μg/mL) of the NP1 sample was observed. No statistical differences were found for the other groups, all of them in comparison to the control group. For 72 h, only the concentration of 5 μg/mL for the NP1 sample showed a statistical difference, presenting a slight increase in the number of viable cells in comparison with the control group.

Figure 4 presents the obtained results for cell viability, when the direct contact of ZnO NPs and the pre-osteoblasts was adopted. In this figure, the symbols * for $p < 0.05$, ** for $p < 0.001$, and *** for $p < 0.0001$ were also adopted.

From the MTT results shown in Fig. 4, it is possible to observe, after 24 h, lower values in cell viability for the lower concentration (5 μg/mL) of the NP2 sample and for the higher concentrations (50 μg/mL) for the NP1, NP2, and NP3 samples and similar values for all the other groups compared with the control group. For 48 h, lower values in cell viability were observed for the intermediate concentration (10 μg/mL) of the NP3 sample and the higher concentration (50 μg/mL) of NP2. Furthermore, a significant decrease in the number of viable cells was observed for the higher concentration (50 μg/mL) of the NP3 sample. No significant differences were observed for the other groups within this period. Finally, for 72 h of the experimental period, only the lower concentration (5 μg/mL) for NP1 presents similar values of cell viability compared with the control and all the other tested concentrations for the NP1,

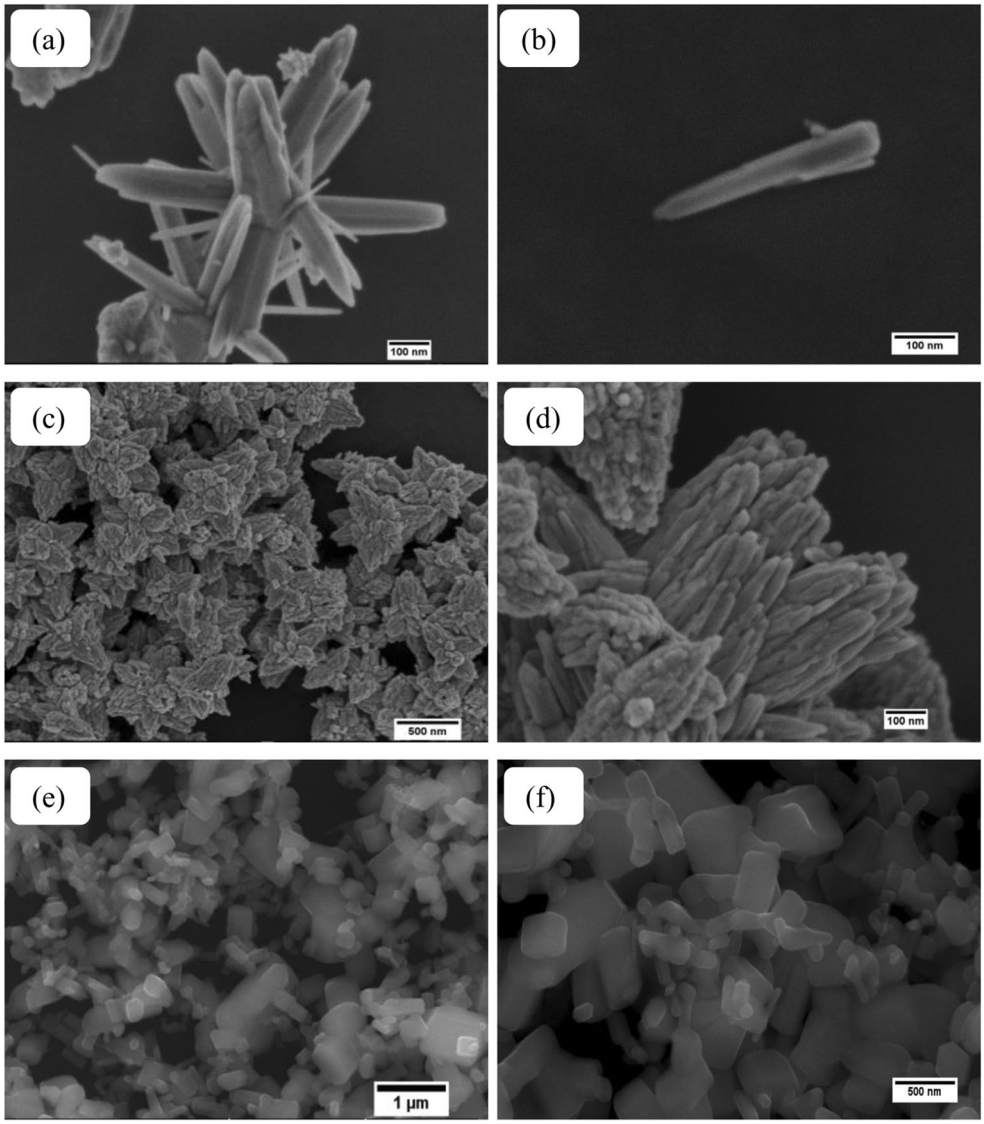

Fig. 2 SEM images for **a** NP1 sample, **b** a single rod of NP1 sample in detail, **c** NP2 sample, **d** NP2 sample in detail, **e** NP3 sample, and **f** NP3 sample in detail

NP2, and NP3 samples showed a decrease in the number of viable cells, mainly the higher concentration (50 μg/mL) for NP3, as observed in 48 h.

4 Discussion

From the XRD patterns (Fig. 1), it was possible to confirm that synthesized ZnO NPS have a pure and hexagonal ZnO crystal structure (indexed by theoretical card JCPDS 36-1451), although with less crystallinity than ZnO commercial powder.

Table 2 Average size for all the samples

Name	Average size (nm)	Standard deviation (nm)
NP1	360	40
NP2	720	100
NP3 (commercial)	560	130

The possible antibacterial property and biological activity regarding living cells of the particles may be associated with how such structures are formed, including the intermediary ionic specimens in solution. Kale and co-workers [40] have previously suggested that the ZnO formation from a zinc salt (as a Zn^{2+} precursor) dissolution in water with the addition of hydroxyl (OH^-) precursor is given by the following reactions:

$$Zn^{2+} + 2(OH)^- \leftrightarrow Zn(OH)_2 \quad (1)$$

$$Zn(OH)_2 + 2(OH)^- \rightarrow Zn(OH)_4^{2-} \quad (2)$$

$$Zn(OH)_4^{2-} \rightarrow ZnO + H_2O + 2OH^- \quad (3)$$

Zak and co-workers [41] have shown that different morphologies may also be obtained from zinc salt water

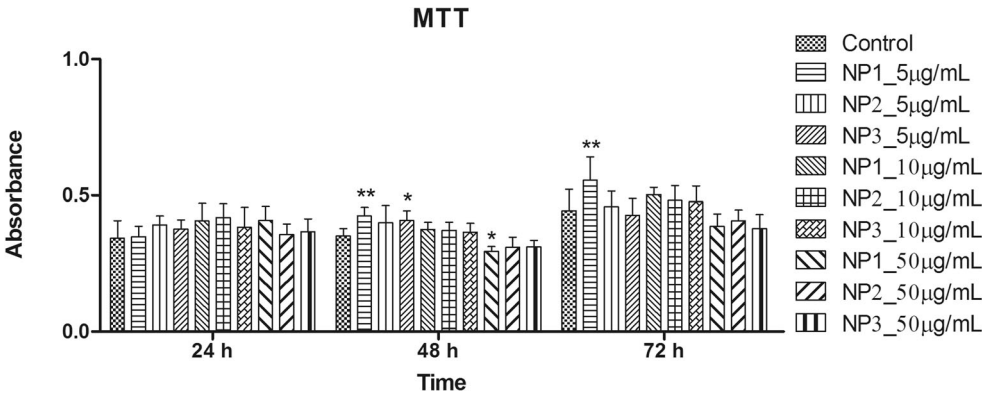

Fig. 3 Cell viability assay (MTT) regarding the ionic cytotoxicity of ZnO NPs (* for $p < 0.05$, ** for $p < 0.001$, and *** for $p < 0.0001$)

dissolution with the addition of a hydroxyl precursor and different sonication times. These authors have obtained ZnO rod-like structures after 15 min of sonication and ZnO flower-like structures after 30 min of sonication, and they believe that the formation mechanism of a flower-like ZnO structure may be due to the action of Coulomb forces over the negatively charged rod-like structures formed during the initial 15 min of sonochemical treatment.

However, previous results from our group indicated that the morphology is more closely related to the precipitation time than to the sonication time [34]. It was demonstrated that flower-like structures may be obtained even without sonochemical treatment and after different sonochemical treatment times when a mixture of zinc nitrate aqueous solution (used as a Zn^{2+} precursor) with ammonium hydroxide addition (for OH^- formation) is left to rest for 24 h. Thus, the Coulomb attraction process of the rod-like structures to form flower-like structures proposed by Zak et al. may occur during the precipitation time. Therefore, for the precipitates immediately collected from solution after sonochemical treatment, there was insufficient time to form flower-like structures. This hypothesis was confirmed by SEM images, as shown in Fig. 2, wherein it is possible to observe rod-like structures for the ZnO sonicated solution with immediately collected precipitates (Fig. 2a, b) and a flower-like morphology for the same sonicated solution wherein the precipitates were collected only after 24 h (Fig. 2c, d).

Considering the cell viability assay performed without direct contact of ZnO NPs with pre-osteoblast cells (Fig. 3), globally, any of the ZnO morphologies seem to have presented cytotoxic effects over MC3T3-E1 pre-osteoblast cell line, and the lower concentration (5 μg/mL) for the NP1 sample (rod-like ZnO particles) apparently favors cell proliferation, as verified by MTT. These results are in accordance with the results found by other authors [42–45].

Concerning the direct contact methodology to test the cell viability of pre-osteoblasts exposed to ZnO NPs, as shown in Fig. 4, it is possible to observe that for most samples, higher concentrations (50 μg/mL) are related to the decrease in the number of viable cells in all the experimental periods, while the intermediate (10 μg/mL) and lower concentrations (5 μg/mL) present no pronounced cytotoxic effects in the first experimental 48 h, except for the intermediate concentration of the NP3 sample.

It is known that zinc is a trace element widely distributed in plants and animal tissues and is present in all living cells. In virtue of being a functional or structural element of more than 300 proteins, zinc is also involved in a considerable number of cellular processes, like enzymatic activity, DNA synthesis,

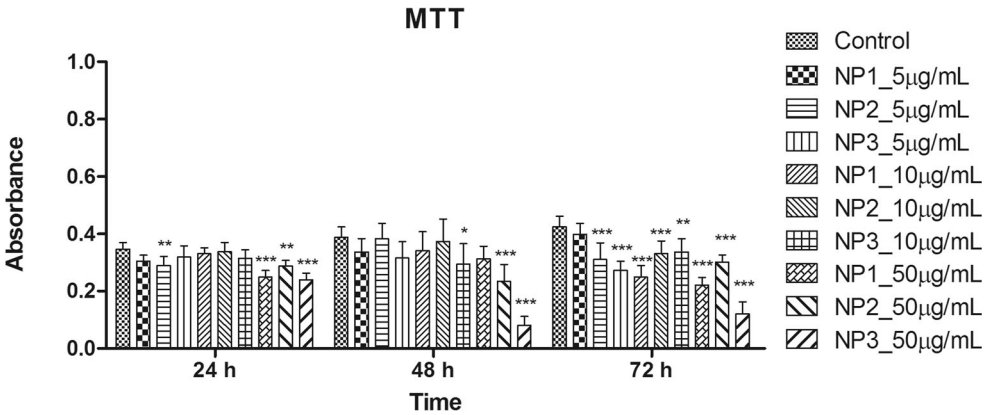

Fig. 4 Cell viability assay (MTT) regarding the direct contact of ZnO nanoparticles with cells (* for $p < 0.05$, ** for $p < 0.001$, and *** for $p < 0.0001$)

and cell division and/or replication. In that sense, it is also believed that zinc may stimulate bone formation by increasing osteogenic function in osteoblasts through exciting cell proliferation, alkaline phosphatase activity, and collagen and protein synthesis [46–49]. Lower concentrations (micromolar) of zinc have been used in a cell culture medium for adequate cellular function [50].

Furthermore, it is widely recognized that due to their small sizes, NPs have a greater surface area than their micro and bulk counterparts, which makes these smaller particles much more chemically reactive. In this work, the NP1 sample has a smaller size and higher chemical surface reactivity than NP2 and NP3 samples. Thus, the zinc ion release rate for this sample is probably higher than for the two others. Therefore, we believe that the increased number of cells observed for the lower concentration (5 μg/mL) of ZnO NP1 sample is related to a suitable balance between the concentration and in the ion release rate from this sample surface.

Taking the decreased number of live cells for all higher concentrations of ZnO NPS in direct contact with cells into account, it is possible that at higher concentrations, ZnO NPs and released ions may be internalized by the pre-osteoblast cells in greater amounts that they can process without interfering in regular metabolism, leading to the cell death [51], even though specific studies to understand the involved mechanisms must be conducted. Saikia and co-workers [52] using different cell lines, showed a linear relationship between ZnO concentration and ROS generation, for example.

In addition, the lower concentration for the NP1 sample presented not only non-cytotoxic behavior, but also a slight proliferative effect in pre-osteoblasts along time, as we have observed when adopting the protocol of non-direct contact with cells, which leads us to believe that there is a suitable balance between concentration size, morphology and, consequently ion releasing rate for this sample, stimulating osteoblast cells to proliferate.

5 Conclusions

Based on the reported results and analyses, the sonochemical method appears to be an efficient technique to produce crystalline ZnO micro and nanoparticles with different morphologies. In addition, the precipitation time after sonochemical treatment of zinc-salt aqueous solutions with the addition of a hydroxyl precursor influences the obtained ZnO morphology.

Regarding the cytotoxicity of the studied samples, the interaction between zinc ionic species and pre-osteoblast may not lead cytotoxic effects; however, the direct contact of these cells with ZnO NPs may induce undesired effects and cell death. Finally, the concentration of 5 μg/mL for ZnO rod-like structures with an average size of 360 ± 40 nm presents a suitable balance between concentration, size, and morphology and, consequently, ion releasing rate regarding pre-osteoblasts.

Funding Information The authors wish to thank CCDPN-SisNano at the Instituto de Química, UNESP – Araraquara, Fundação de Amparo à Pesquisa do Estado de São Paulo – FAPESP (2013/07296-2), Coordenação de Aperfeiçoamento de Pessoal de Nível Superior – CAPES (99999.008666/2014-08), and Conselho Nacional de Desenvolvimento Científico e Tecnológico – CNPq (490761/2013-5) for their financial support.

References

1. Janotti, A., & van De Walle, C. G. (2009). Fundamentals of zinc oxide as a semiconductor. *Reports on Progress in Physics, 72*, 126501. https://doi.org/10.1088/0034-4885/72/12/126501.
2. Fang, F., Kennedy, J., Carder, D. A., Futter, J., Murmu, P., & Markwitz, A. (2010). Modulation of field emission properties of ZnO nanorods during arc discharge. *Journal of Nanoscience and Nanotechnology, 10*, 8239–8243. https://doi.org/10.1166/jnn.2010.3009.
3. Applerot, G., Lipovsky, A., Dror, R., Perkas, N., Nitzan, Y., Lubart, R., & Gedanken, A. (2009). Enhanced antibacterial activity of nanocrystalline ZnO due to increased ROS-mediated cell injury. *Advanced Functional Materials, 19*(6), 842–852. https://doi.org/10.1002/adfm.200801081.
4. Silva-Bermudez, P., & Rodil, S. E. (2013). An overview on protein adsorption on metal oxide coatings for biomedical implants. *Surface and Coating Technology, 233*, 147–158. https://doi.org/10.1016/j.surfcoat.2013.04.028.
5. Hong, H., Shi, J., Yang, Y., Zhang, Y., Engle, J. W., Nickles, R. J., Wang, X., & Cai, W. (2011). Cancer-targeted optical imaging with fluorescent zinc oxide nanowires. *Nano Letters, 11*(9), 3744–3750. https://doi.org/10.1021/nl201782m.
6. Zhang, H., Chen, B., Jiang, H., Wang, C., Wang, H., & Wang, X. (2011). A strategy for ZnO nanorod mediated multi-mode cancer treatment. *Biomaterials, 32*(7), 1906–1914. https://doi.org/10.1016/j.biomaterials.2010.11.027.
7. Wang, H., Wingett, D., Engelhard, M. H., Feris, K., Reddy, K. M., Turner, P., Layne, J., Hanley, C., Bell, J., Tenne, D., Wang, C., & Punnoose, A. (2009). Fluorescent dye encapsulated ZnO particles with cell-specific toxicity for potential use in biomedical applications. *Journal of Materials Science - Materials in Medicine, 20*(1), 11–22. https://doi.org/10.1007/s10856-008-3541-z .
8. Zhou, J., Xu, N., & Wang, Z. L. (2006). Dissolving behavior and stability of ZnO wires in biofluids: a study on biodegradability and biocompatibility of ZnO nanostructure. *Advanced Materials, 18*, 2432–2435. https://doi.org/10.1002/adma.200600200.
9. Shepherd, J., Shepherd, D., & Best, S. (2012). Substituted hydroxyapatites for bone repair. *Journal of Materials Science - Materials in Medicine, 23*(10), 2335–2347. https://doi.org/10.1007/s10856-012-4598-2 .
10. Li, M. O., Xiao, X., Liu, R., & Chen, H. L. (2008). Structural characterization of zinc-substituted hydroxyapatite prepared by hydrothermal method. *Journal of Materials Science - Materials in Medicine, 19*(2), 797–803. https://doi.org/10.1007/s10856-007-3213-4 .
11. You, C., Han, C., Wang, X., Zheng, Y., Li, Q., Hu, X., & Sun, H. (2012). The progress of silver nanoparticles in the antibacterial mechanism, clinical application and cytotoxicity. *Molecular Biology Reports, 39*(9), 9193–9201. https://doi.org/10.1007/s11033-012-1792-8.
12. Goodman, S. B., Yao, Z., Keeney, M., & Yang, F. (2013). The future of biologic coatings for orthopaedic implants. *Biomaterials,*

34(13), 3174–3183. https://doi.org/10.1016/j.biomaterials.2013.01.074.

13. Chen, W., Liu, Y., Courtney, H. S., Bettenga, M., Agrawal, C. M., Bumgardner, J. D., & Ong, J. L. (2006). In vitro anti-bacterial and biological properties of magnetron co-sputtered silver-containing hydroxyapatite coating. *Biomaterials, 27*(32), 5512–5517. https://doi.org/10.1016/j.biomaterials.2006.07.003 .
14. Chen, Q., & Thouas, G. A. (2015). Metallic implants biomaterials. *Materials Science and Engineering R, 87*, 1–57. https://doi.org/10.1016/j.mser.2014.10.001.
15. Albers, C. E., Hofstetter, W., Siebenrock, K. A., Landmann, R., & Klenke, F. M. (2013). In vitro cytotoxicity of silver nanoparticles on osteoblasts and osteoclasts at antibacterial concentrations. *Nanotoxicology, 7*(1), 30–36. https://doi.org/10.3109/17435390.2011.626538.
16. Liu, W., Wu, Y., Wang, C., Li, H. C., Wang, T., Liao, C. Y., Cui, L., Zhou, Q. F., Yan, B., & Jiang, G. B. (2010). Impact of silver nanoparticles on human cells: effect of particle size. *Nanotoxicology, 4*(3), 319–330. https://doi.org/10.3109/17435390.2010.483745.
17. Song, W., Zhang, J., Guo, J., Zhang, J., Ding, F., Li, L., & Sun, Z. (2010). Role of the dissolved zinc ion and reactive oxygen species in cytotoxicity of ZnO nanoparticles. *Toxicology Letters, 199*, 389–397. https://doi.org/10.1016/j.toxlet.2010.10.003.
18. Sirelkhatim, A., Mahmud, S., Seeni, A., Haida, N., Kaus, M., Ann, L., Bakhori, S. K. M., Hasan, H., & Mohamad, D. (2015). Review on zinc oxide nanoparticles: antibacterial activity and toxicity mechanism. *Nano-Micro Letters, 7*(3), 219–242. https://doi.org/10.1007/s40820-015-0040-x .
19. Lemire, J. A., Harrison, J. J., & Turner, R. J. (2013). Antimicrobial activity of metals: mechanisms, molecular targets and applications. *Nature Reviews. Microbiology, 11*(6), 371–384. https://doi.org/10.1038/nrmicro3028.
20. Xie, Y., He, Y., Irwin, P. L., Jin, T., & Shi, X. (2011). Antibacterial activity and mechanism of action of zinc oxide nanoparticles against Campylobacter jejuni. *Applied and Environmental Microbiology, 77*(7), 2325–2331. https://doi.org/10.1128/AEM.02149-10.
21. Heng, B. C., Zhao, X., Tan, E. C., Khamis, N., Assodani, A., Xiong, S., Ruedl, C., Ng, K. W., & Loo, J. S. (2011). Evaluation of the cytotoxic and inflammatory potential of differentially shaped zinc oxide nanoparticles. *Archives of Toxicology, 85*, 1517–1528. https://doi.org/10.1007/s00204-011-0722-1.
22. Yang, H., Liu, C., Yang, D., Zhang, H., & Xi, Z. (2009). Comparative study of cytotoxicity, oxidative stress and genotoxicity induced by four typical nanomaterials: the role of particle size, shape and composition. *Journal of Applied Toxicology, 29*, 69–78. https://doi.org/10.1002/jat.1385.
23. Thian, E. S., Konishi, T., Kawanobe, Y., Lim, P. N., Choong, C., Ho, B., & Aizawa, M. (2013). Zinc-substituted hydroxyapatite: a biomaterial with enhanced bioactivity and antibacterial properties. *Journal of Materials Science - Materials in Medicine, 24*(2), 437–445. https://doi.org/10.1007/s10856-012-4817-x .
24. Yang, F., Dong, W. J., He, F. M., Wang, X. X., Zhao, S. F., & Yang, G. L. (2012). Osteoblast response to porous titanium surfaces coated with zinc-substituted hydroxyapatite. *Oral Surgery, Oral Medicine, Oral Pathology, Oral Radiology, 113*(3), 313–318. https://doi.org/10.1016/j.tripleo.2011.02.049.
25. Shepherd, D. V., Kauppinen, K., Brooks, R. A., & Best, S. M. (2014). An in vitro study into the effect of zinc substituted hydroxyapatite on osteoclast number and activity. *Journal of Biomedical Materials Research. Part A, 102*(11), 4136–4141. https://doi.org/10.1002/jbm.a.35089.
26. Hu, H., Zhang, W., Qiao, Y., Jiang, X., Liu, X., & Ding, C. (2012). Antibacterial activity and increased bone marrow stem cell functions of Zn-incorporated TiO_2 coatings on titanium. *Acta Biomaterialia, 8*(2), 904–915. https://doi.org/10.1016/j.actbio.2011.09.031.
27. Jung, S. H., Oh, E., Lee, K. H., Yang, Y., Park, C. G., Park, W., & Jeong, S. H. (2008). Sonochemical preparation of shape-selective ZnO nanostructures. *Crystal Growth & Design, 8*(1), 265–269. https://doi.org/10.1021/cg0702961.
28. Suslick, K. S., & Price, G. J. (1999). Applications of ultrasound to materials chemistry. *Annual Review of Materials Research, 29*, 295–326. https://doi.org/10.1146/annurev.matsci.29.1.295.
29. Mason, T. J., & Lorimer, J. P. (1989). An introduction to sonochemistry. *Endeavour, 13*(3), 123–128. https://doi.org/10.1016/0160-9327(89)90086-0.
30. Pholnak, C., Sirisathitkul, C., & Harding, D. J. (2011). Characterizations of octahedral zinc oxide synthesized by sonochemical method. *Journal of Physics and Chemistry of Solids, 72*(6), 817–823. https://doi.org/10.1016/j.jpcs.2011.04.005.
31. Pu, X. P., Zhang, D. F., Jia, L. P., & Su, C. H. (2007). Synthesis of zinc oxide nanostructures with controlled morphologies using a simple sonochemical method. *Journal of the American Ceramic Society, 90*(12), 4076–4078. https://doi.org/10.1111/j.1551-2916.2007.02084.x.
32. Chen, S., Kumar, R. V., Gedanken, A., & Zaban, A. (2001). Sonochemical synthesis of crystalline nanoporous zinc oxide spheres and their application in dye sensitized solar cells. *Israel Journal of Chemistry, 41*(1), 51–54. https://doi.org/10.1560/HQ1V-8KAG-5KQK-E91F.
33. Arruda, L. B., Orlandi, M. O., & Lisboa-Filho, P. N. (2013). Morphological modifications and surface amorphization in ZnO sonochemically treated nanoparticles. *Ultrasonics Sonochemistry, 20*(3), 799–804. https://doi.org/10.1016/j.ultsonch.2012.11.013.
34. Costa, B. C., Morilla-Santos, C., & Lisboa-Filho, P. N. (2015). Effects of time exposure and low power sonochemical treatment on ZnO mesostructures. *Materials Science in Semiconductor Processing, 35*, 81–89. https://doi.org/10.1016/j.mssp.2015.02.058.
35. Volpato, L. E. R., Oliveira, R. C., Espinosa, M. M., Bagnato, V. S., & Machado, M. A. A. M. (2011). Viability of fibroblasts cultured under nutritional stress irradiated with red laser, infrared laser, and red light-emitting diode. *Journal of Biomedical Optics, 16*(7), 075004–075001. https://doi.org/10.1117/1.3602850.
36. Machado, A. C., Souza, L. P., Saldanha, L. L., Pieroni, L. G., Matos, A. A., Oliveira, F. A., Vilegas, W., Damante, C. A., Dokkedal, A. L., & Oliveira, R. C. (2016). "Aroeira" (Myracrodruon urundeuva) methanol extract: the relationship between chemical compounds and cellular effects. *Pharmaceutical Biology, 54*(11), 2737–2741. https://doi.org/10.1080/13880209.2016.1182555.
37. Scelza, M. Z., Linhares, A. B., da Silva, L. E., Granjeiro, J. M., & Alves, G. G. (2012). A multi parametric assay to compare the cytotoxicity of endodontic sealers with primary human osteoblasts. *International Endodontic Journal, 45*(1), 12–18. https://doi.org/10.1111/j.1365-2591.2011.01941.x .
38. International Organization for Standardization (2009) ISO 10993-5: biological evaluation of medical devices—part 5: tests for in vitro cytotoxicity. ISO 10993-5:2009 ed.
39. International Organization for Standardization (2012) ISO 10993-12: biological evaluation of medical devices—part 12: sample preparation and reference materials. ISO 10993-12:2012 ed.
40. Kale, R. B., Hsu, Y. J., Lin, Y. F., & Lu, S. Y. (2014). Hydrothermal synthesis, characterizations and photoluminescence study of single crystalline hexagonal ZnO nanorods with three dimensional flower-like microstructures. *Superlattices and Microstructures, 69*, 239–252. https://doi.org/10.1016/j.spmi.2014.03.003.
41. Zak, A. K., Majid, W. H., Wang, H. Z., Yousefi, R., Golsheikh, A. M., & Ren, Z. F. (2013). Sonochemical synthesis of hierarchical

ZnO nanostructures. *Ultrasonics Sonochemistry, 20*, 395–400. https://doi.org/10.1016/j.ultsonch.2012.07.001.

42. Choudhury, S. R., Ordaz, J., Lo, C. L., Damayanti, N. P., Zhou, F., & Irudayaraj, J. (2017). ZnO nanoparticles induced reactive oxygen species promotes multimodal cyto- and epigenetic toxicity. *Toxicological Sciences, 156*(1), 261–274. https://doi.org/10.1093/toxsci/kfw252.
43. Salari, Z., Ameri, A., Forootanfar, H., Adeli-Sardou, M., Jafari, M., Mehrabani, M., & Shakibaie, M. (2017). Microwave-assisted biosynthesis of zinc nanoparticles and their cytotoxic and antioxidant activity. *Journal of Trace Elements in Medicine and Biology, 39*, 116–123. https://doi.org/10.1016/j.jtemb.2016.09.001.
44. Soni, D., Gandhi, D., Tarale, P., Bafana, A., Pandey, R. A., & Sivanesan, S. (2017). Oxidative stress and genotoxicity of zinc oxide nanoparticles to pseudomonas species, human promyelocytic leukemic (HL-60), and blood cells. *Biological Trace Element Research, 178*(2), 218–227. https://doi.org/10.1007/s12011-016-0921-y.
45. El Yamani, N., Collins, A. R., Rundén-Pran, E., Fjellsbø, L. M., Shaposhnikov, S., Zielonddiny, S., & Dusinska, M. (2017). In vitro genotoxicity testing of four reference metal nanomaterials, titanium dioxide, zinc oxide, cerium oxide and silver: towards reliable hazard assessment. *Mutagenesis, 32*(1), 117–126. https://doi.org/10.1093/mutage/gew060.
46. Kononenko, V., Repar, N., Marušič, N., Drašler, B., Romih, T., Hočevar, S., & Drobne, D. (2017). Comparative in vitro genotoxicity study of ZnO nanoparticles, ZnO macroparticles and $ZnCl_2$ to MDCK kidney cells: size matters. *Toxicology In Vitro, 40*, 256–263. https://doi.org/10.1016/j.tiv.2017.01.015.
47. Valko, M., Morris, H., & Cronin, M. T. (2005). Metals, toxicity and oxidative stress. *Current Medicinal Chemistry, 12*, 1161–1208. https://doi.org/10.2174/0929867053764635.
48. Soetan, K. O., Olaiya, C. O., & Oyewole, O. E. (2010). The importance of mineral elements for human, domestic animals and plants: a review. *African Journal of Food Science, 4*(5), 200–222.
49. Jin, G., Cao, H., Qiao, Y., Meng, F., Zhu, H., & Liu, X. (2014). Osteogenic activity and antibacterial effect of zinc ion implanted titanium. *Colloids and Surfaces B - Biointerfaces, 117*, 168–165. https://doi.org/10.1016/j.colsurfb.2014.02.025 .
50. Freshney, R. I. (2010. 732 p.). *Culture of animal cells: a manual of basic technique and specialized applications. 6. Eed.* Hoboken: Wiley-Blackwell.
51. Kaviyarasu, K., Geetha, N., Kanimozhi, K., Maria Magdalane, C., Sivaranjani, S., Ayeshamariam, A., Kennedy, J., & Maaza, M. (2017). In vitro cytotoxicity effect and antibacterial performance of human lung epithelial cells A549 activity of Zinc oxide doped TiO_2 nanocrystals: investigation of bio-medical application by chemical method. *Materials Science and Engineering C - Materials for Biological Applications, 74*, 325–333. https://doi.org/10.1016/j.msec.2016.12.024.
52. Saikia, C., Das, M. K., Ramteke, A., & Maji, T. K. (2017). Evaluation of folic acid tagged aminated starch/ZnO coated iron oxide nanoparticles as targeted curcumin delivery system. *Carbohydrate Polymers, 157*, 391–399. https://doi.org/10.1016/j.carbpol.2016.09.087.